THE FORMATION OF ULTRAFINE GRAINED MICROSTRUCTURE IN A PLAIN C-MN STEEL

Rongjie Song; Dirk Ponge; Dierk Raabe
Max-Planck-Institut für Eisenforschung, Max-Planck-Str. 1, 40237 Düsseldorf, Germany

ABSTRACT

A plain C-Mn steel with ultrafine ferrite grains (average grain size of 1.3 μm) and homogeneously distributed cementite particles was produced by large strain warm deformation (ε = 1.6) and subsequent annealing. The ultrafine microstructures were stable against grain and particle coarsening even during a 2 h annealing treatment at 823 K. We observed a critical strain of ~0.8 which was required as a lower bound for efficiently refining the microstructure. A further increase in strain over this value is beneficial for the formation of a higher fraction of high-angle grain boundaries and more equiaxed ferrite grains. The grain refinement by large strain warm deformation is explained in terms of a continuous recrystallization process. Deformation induced grain subdivision is essential for the formation of ultrafine grains. Spheroidization of pearlitic cementite lamellae during the large strain warm deformation is assumed to be accelerated by the fragmentation of cementite lamellae and the formation of subgrain boundaries in ferrite. During the deformation-annealing cycle, the fine cementite particles may dissolve and carbon in solid solution can diffuse from the areas of the former pearlite colonies to the cementite free areas inside the former pro-eutectoid ferrite followed by subsequent re-precipitation and competitive coarsening. A homogeneous distribution of cementite particles was obtained after the deformation-annealing treatment.

KEYWORDS

Steel; EBSD; recrystallization; recovery; ultrafine grains; spheroidization; re-precipitation

INTRODUCTION

Among the different strengthening mechanisms, grain refinement is the only method to improve both strength and toughness simultaneously. Therefore, ultrafine grained steels with relatively simple chemical compositions, strengthened primarily by grain refinement, have great potential for replacing alloyed high strength steels. The main benefits behind such a strategy are to avoid additional alloying elements, to skip complicated additional heat treatments like soft annealing, quenching and tempering, and to improve weldability owing to the reduced required content of carbon and other alloying elements when compared with high strength quenched and tempered steels. A further high potential area of ultrafine grained steels is the domain of high strain rate superplasticity at medium and elevated temperatures [1–4].

In general, the term ultrafine grain is used for average grain sizes between 1 μm and 2 μm in diameter; the term submicron structure refers to grain sizes between 100 nm and 1000 nm; and the term nano-structure means grain sizes below 100 nm.

In this study, we introduce a new concept for producing ultrafine grained C–Mn steel by thermomechanical processing. In particular, a considerable effort was made to understand the

details of the evolution of microstructure during the large strain warm deformation and subsequent annealing treatment by using field-emission scanning electron microscopy (FE-SEM) and high resolution electron backscatter diffraction (EBSD). The influence of the fine cementite particles on the formation of ultrafine microstructures and in particular on the recovery process were studied by use of transmission electron microscopy (TEM).

By studying the key mechanisms associated with the formation of ultrafine grained microstructures in the course of the thermomechanical routes investigated in this work we hope to develop well tailored and microstructurally guided approaches to the large scale production of ultrafine grained steels.

EXPERIMENTAL METHODS

The chemical composition of the C–Mn steel used in this work was 0.22C–0.21Si–0.74Mn–0.004P–0.003S–0.001N–0.029Al (mass%). The laboratory samples were machined directly from the cast ingot into rectangular parallelepiped samples of 50 × 40 × 60 mm^3 (width × length × height). The plane strain compression tests were conducted by use of a large scale 2.5 MN hot press [5], where the compression direction was parallel to the sample height.

After reheating with a heating rate of 10 K/s, the samples were austenitized at 1193 K for 3 minutes. After air cooling to 1143 K, a one-step deformation pass was exerted imposing a logarithmic strain of $\varepsilon = 0.3$ at a strain rate of 10 s^{-1}. This was followed by a controlled cooling procedure down to the pearlite finish temperature of 823 K at a cooling rate of 6.5 K/s. After this primary treatment which was identical for all specimens, the following different experimental routes were carried out to provide sets of different sample states:

a) Ultrafine grain route: After a 2 minutes holding period at 823 K, the large strain warm deformation was performed by applying a four-pass plane strain compression process at 823K with an inter-pass time of 0.5 s. Each of the four subsequent steps imposed a logarithmic strain of $\varepsilon = 0.4$ accumulating to a total strain of $\varepsilon = 1.6$. Each pass was conducted at a strain rate of 10 s^{-1}. Subsequently, an annealing treatment of 2 hours at 823 K was exerted.

b) Route for studying microstructure evolution during warm deformation: In order to study the details of the evolution of the ultrafine microstructure in the course of the large strain warm deformation procedure, samples were water quenched after intermediate true accumulated strains of $\varepsilon = 0$, 0.4, 0.8, 1.2, and 1.6, respectively.

The microstructure characteristics of the specimens were investigated by use of light optical microscopy, high resolution SEM, EBSD, and TEM. High-angle grain boundaries (HAGB) are homophase interfaces with a misorientation angle of $\theta \geq 15°$. Lower values of the local misorientation ($15° > \theta \geq 2°$) represent low-angle grain boundaries (LAGB). The grain shape aspect ratio of each grain was defined as the grain length measured in the rolling direction (RD) divided by that measured in the normal direction (ND).

EXPERIMENTAL RESULTS

Evolution of microstructure during warm deformation

Figs. 1 and 2 document the microstructure evolution of the steel during deformation and subsequent annealing. Fig. 1a shows the initial ferrite-pearlite microstructure before the warm deformation. Figs. 1b and 3a show that the ferrite-pearlite microstructure was finer after the first deformation step (ε = 0.4) than before the warm deformation. Also, the grains are elongated in the rolling direction. Although the ferrite grain boundaries are clearly visible in Fig. 1b after the first warm deformation step of ε = 0.4, many details of a faint substructure appear as fine lines inside some of the ferrite grains.

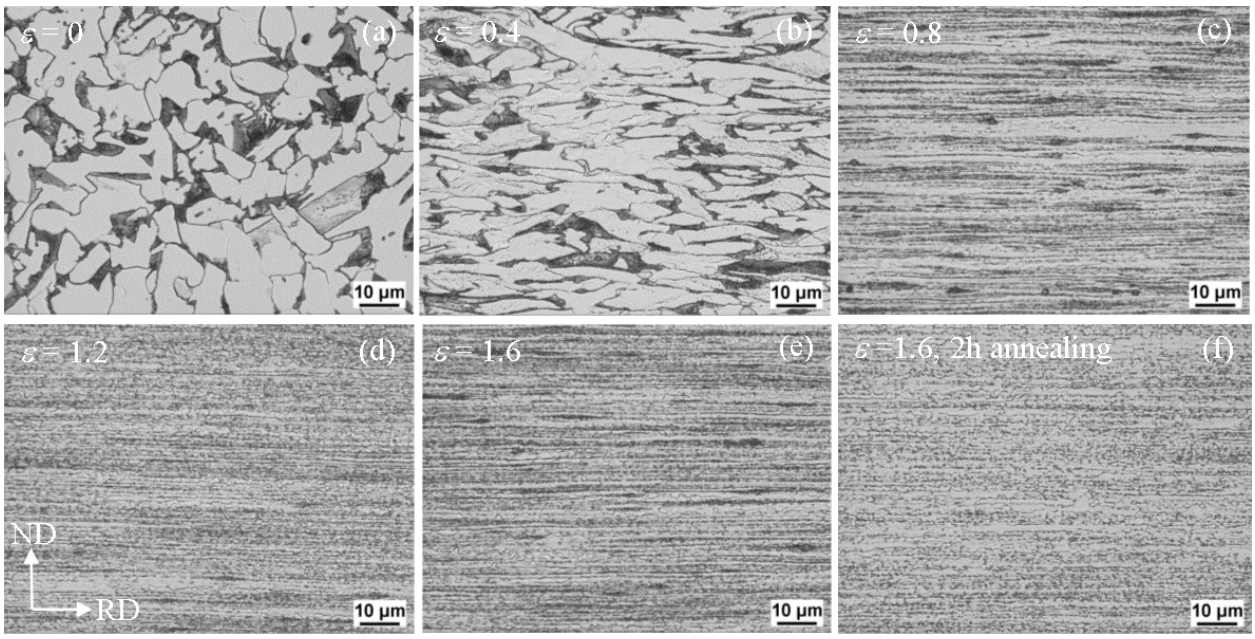

Fig. 1 Optical microstructures of the steel during warm deformation and subsequent annealing at 823 K. (a) initial microstructure before large strain warm deformation; (b)–(e) microstructures after one to four deformation steps (ε = 0.4, 0.8, 1.2 and 1.6), respectively; (f) microstructure after four deformation steps and a subsequent 2 h annealing treatment at 823 K.

After the second deformation step (ε = 0.8) the microstructure is too fine to be resolved by optical microscopy, Fig. 1c. A higher magnification (see SEM image, Fig. 2b) reveals that the microstructure consists of ferrite and partially spheroidized cementite. The former pearlite colonies are elongated and can still be clearly distinguished. The fraction of high-angle grain boundaries decreases, Fig. 3b.

After the third deformation step (ε = 1.2) the average ferrite grain size decreases slightly and the grain shape aspect ratio remains practically unchanged, Fig. 3a. On the other hand, the fraction of high-angle grain boundaries has increased, Figs. 3b.

Most of the pearlite lamellae were spheroidized into cementite particles after four deformation steps (ε = 1.6), Fig. 2c. The clear alignments of the cementite particles which decorate the ferrite grain boundaries still can be seen (arrow “1”). Different sizes of cementite particles (arrows “1” and “2”) and cementite fragments (arrow “3”) were inhomogeneously distributed within the ferrite matrix. The ferrite grain size decreases and the grain shape becomes more equiaxed with increasing strain, Fig. 3a. The fraction of high-angle grain boundaries remains practically unchanged, Fig. 3b.

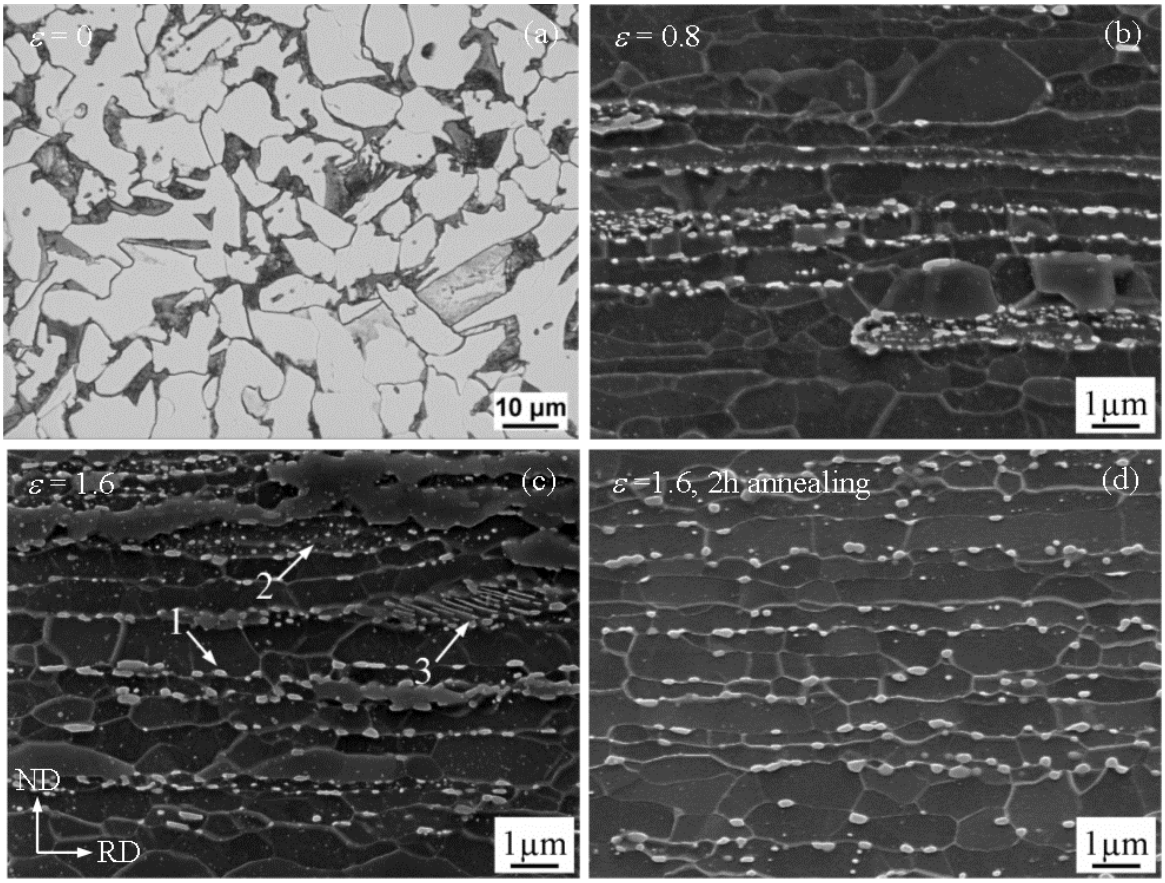

Fig. 2 Microstructural evolution of the steel during warm deformation and subsequent annealing at 823 K. Arrow "1" points at a large cementite particle at a ferrite grain boundary. Arrow "2" points at small cementite particles in the initial pearlite colony region. Arrow "3" points at a cementite lamella in the initial pearlite colony region. (a) initial microstructure before large strain warm deformation; (b) and (c) microstructures after two and four deformation steps (ε = 0.8, 1.6), respectively; (d) microstructure after four deformation steps and a subsequent 2 h annealing treatment at 823 K.

Microstructure after annealing

After annealing the samples (processed by four deformation steps ε = 1.6) for 2 h, there is nearly no change in the grain size. However, the grain shape becomes more equiaxed after that heat treatment, Fig. 3a. Nearly all cementite fragments are spheroidized into globular particles and homogeneously distributed in the ferrite matrix, Fig. 2d. The fraction of high-angle grain boundaries hardly changes during annealing, Fig. 3b.

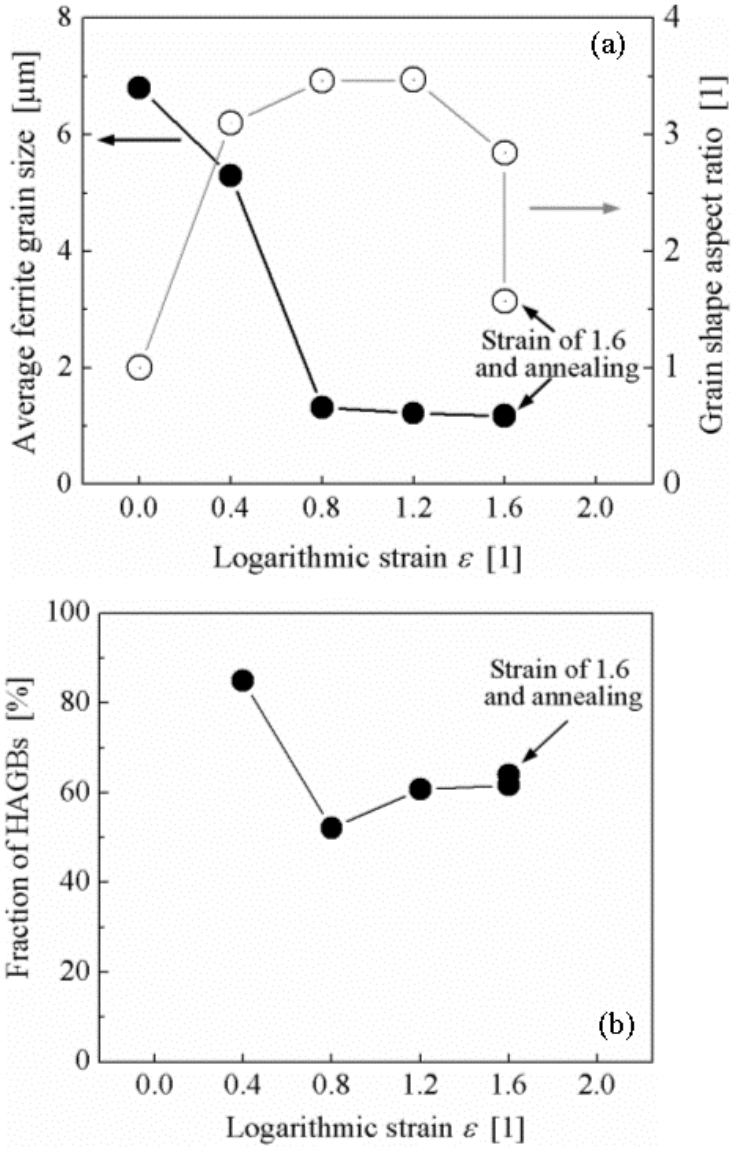

Fig. 3 Evolution of the grain characteristics of the steel during warm deformation and subsequent annealing at 823 K. Each deformation step imposed a true strain of $\varepsilon = 0.4$ at a strain rate of 10 s^{-1}. (a) average ferrite grain size and grain shape aspect ratio; (b) fraction of high-angle grain boundaries (HAGBs).

Evolution of pearlitic cementite lamellae during warm deformation

During warm deformation the increase in strain leads to an alignment of the pearlitic cementite lamellae and, at a later stage, to an alignment of cementite strings. This entails anisotropic growth of the ferrite grains.

TEM analysis

The TEM micrographs of the steel after large strain warm deformation and direct water cooling are shown in Fig. 4a, and after large strain warm deformation followed by a subsequent annealing in Fig. 4b. All microstructures are characterized by ultrafine ferrite grains and globular cementite. The ferrite grain size hardly changed during the post-deformation heat treatment (Fig. 4b), if compared to that observed directly after large strain warm deformation (Fig. 4a). A slight coarsening of the cementite particles occurs after the annealing. Two different size groups of cementite particles can be observed in the microstructure (Fig. 4b). The finer cementite particles (5–90 nm) are distributed

inside the ferrite grains (see arrows 1). The planar arrays of larger cementite particles (90–350 nm) are located at the ferrite grain boundaries (see arrows 2), acting as obstacles impeding their migration. Figs. 4c and d show the dislocation structures in the steel after large strain warm deformation and annealing, respectively. Dislocations were found in both, deformed and annealed samples. The black arrows in Fig. 4d point at cementite particles as they pin dislocations.

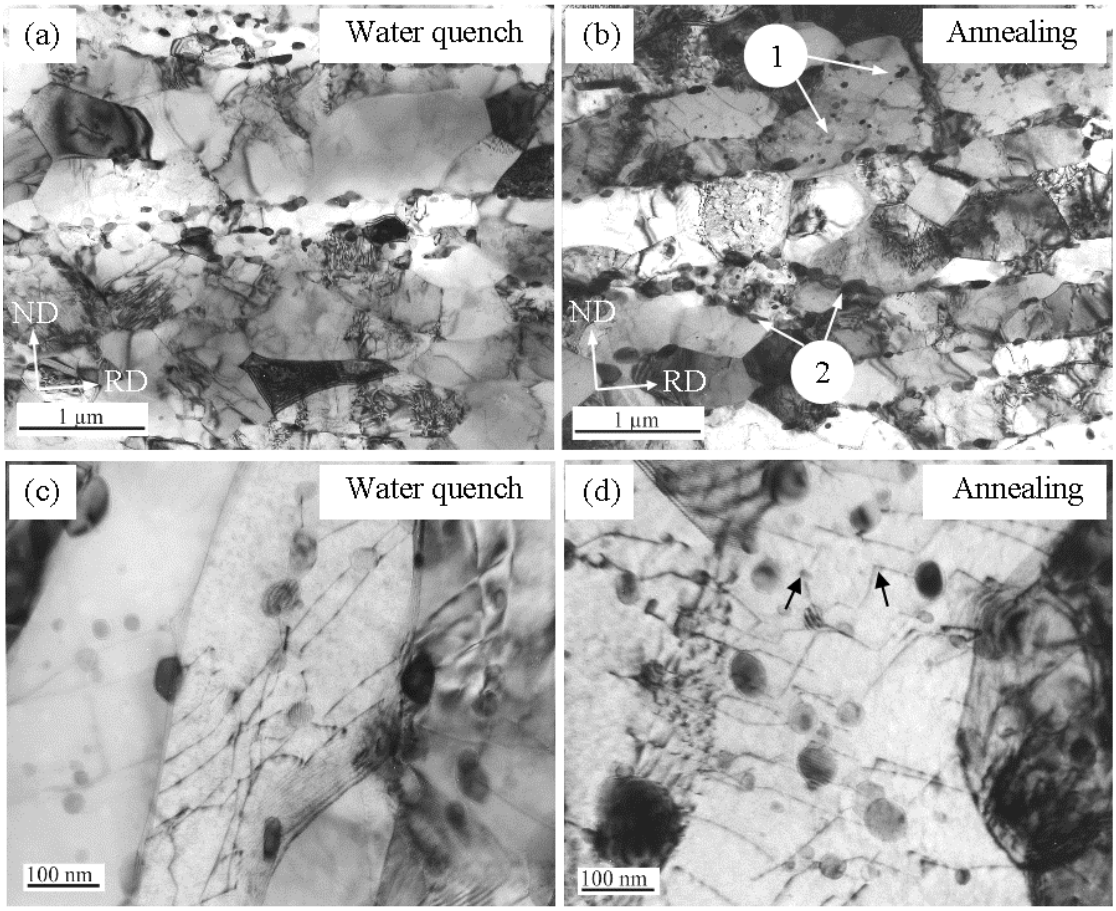

Fig. 4 TEM micrographs of the steel after large strain warm deformation ($\varepsilon = 1.6$) and a subsequent 2h annealing process at 823 K. Arrows "1" point at the fine cementite particles inside the ferrite grains. Arrows "2" point at the coarse cementite particles at the ferrite grain boundaries. (a) and (c) deformed microstructure; (b) and (d) annealed microstructure.

DISCUSSION

Microstructural evolution of the ferrite during large strain warm deformation

Figs. 1 and 3a suggest a critical strain of about 0.8 for refining the initial ferrite-pearlite microstructure. Such a threshold value was also reported by Shin and Apps [6,7] for a low carbon steel and for an Al-Mg alloy which were both processed by severe plastic deformation. As reported by Tsuji [8], in-grain subdivision is of great importance for grain refinement especially when starting from an initially coarse microstructure. Both, the appearance of a more equiaxed grain structure after the large strain deformation and the notable increase in the fraction of high-angle grain boundaries after this threshold strain (Fig. 3b) can be attributed to pronounced recovery, especially to polygonization. Since this process leads in the end to a high fraction of high-angle

grain boundaries (but without the preceding motion of high-angle grain boundaries) it can also be referred to as continuous recrystallization or, equivalently, as recrystallization in-situ [9].

This interpretation is supported by two facts. First, the ferrite grain structures observed are elongated, i.e. the grain shape aspect ratio was about 2.8 after a true strain of ε = 1.6, Fig. 3a. Second, numerous dislocations can be identified inside the grains, Fig. 4c.

During the large strain warm deformation a further increase in strain above the effective value is beneficial for the formation of high-angle grain boundaries and for the adjustment of the grain shape. It can be concluded that the process of gradual deformation-induced crystallite subdivision is the essential process for the formation of an ultrafine grained microstructure. In particular continuous recrystallization is a prerequisite to form high-angle grain boundaries.

Microstructure evolution of the ferrite during annealing

After 2 h annealing at 823 K, numerous dislocations can still be identified inside the grains, Fig. 4d. Compared with the microstructure after the large strain deformation there is a minor change in the fraction of high-angle grain boundaries during annealing (Fig. 3b). These phenomena suggest that a pronounced recovery or respectively extended recovery [10] occurs during the annealing.

Spheroidization of lamellar pearlite

The rate of cementite spheroidization can be enhanced by six orders of magnitude through warm deformation as compared to a stand-alone annealing treatment [11]. The appearance of a former pearlitic cementite lamellae structure is emphasized by arrow “3” in Fig. 2c after a large accumulated strain of 1.6. This observation indicates that the spheroidization is not fully finished after the large strain warm deformation. The distribution of small spheroidized cementite particles in the initial pearlite colony (arrow “2” in Fig. 2c) as well as the alignments of the cementite particles which decorate the ferrite grain boundaries (arrow “1”) indicate that the mere large strain warm deformation process *without* a subsequent annealing is insufficient for a homogeneous distribution of cementite particles.

Distribution of cementite particles

Apart from the processes of spheroidization and coarsening of the cementite, the process of a homogeneous distribution of cementite after the spheroidization can be observed in the present ferrite-pearlite steel after annealing, Fig. 2d. This means that after the large strain warm deformation and subsequent annealing treatment cementite particles can also be found even within the former pro-eutectoid ferrite regions. The redistribution of cementite particles during annealing can be interpreted in terms of a dissolution and re-precipitation mechanism [12].

CONCLUSIONS

A plain C-Mn steel with ultrafine ferrite grains (average grain size of 1.3 µm) and homogeneously distributed cementite particles was produced by large strain warm deformation (ε = 1.6) and subsequent annealing. The ultrafine microstructures were stable against grain and particle coarsening even during a 2 h annealing treatment at 823 K. We observed a critical strain of ~0.8 which was required as a lower bound for efficiently refining the microstructure. A further increase in strain over this value is beneficial for the formation of a higher fraction of high-angle grain

boundaries and the adjustment of the ferrite grains towards a more spherical shape. The basic results and conclusions are given in the following:

1) The grain refinement by large strain warm deformation was explained in terms of a continuous recrystallization process. Deformation induced grain subdivision is essential for the formation of ultrafine grains.

2) During a 2 h heat treatment at 823 K after the large strain deformation procedure grain growth was suppressed. Pronounced recovery at this stage together with the presence of fine carbides suppressing discontinuous recrystallization facilitated the formation of high-angle grain boundaries and the evolution of a more equiaxed grain shape.

3) Spheroidization of pearlitic cementite lamellae during the large strain warm deformation was assumed to be accelerated by fragmentation of cementite lamellae and by the assistance of pipe diffusion. During the deformation-annealing cycle, the fine cementite particles may dissolve and solute carbon then diffuses from the areas of the former pearlite colonies to the cementite free areas inside the former pro-eutectoid ferrite followed by subsequent re-precipitation and competitive coarsening.

REFERENCES

1) R. SONG, D. PONGE, R. KASPAR and D. RAABE, Zeitschrift für Metallkunde 95, (2004), p.513.
2) R. SONG, D. PONGE and D. RAABE, Scripta Mate. 52, (2005), p.1075.
3) R. SONG, R. KASPAR, D. PONGE and D. RAABE, Ultrafine Grained Materials III,TMS 2004, North Carolina,USA (2004), p 445.
4) R. SONG, D. PONGE and R. KASPAR, Steel Research 75, (2004), p.33.
5) R. KASPAR and O. PAWELSKI, Materialprüfung 31, (1989), p.14.
6) D.H. SHIN, B.C. KIM, Y.S. KIM and K.T. PARK, Acta Mater. 48, (2000), p.2247.
7) P.J. APPS, J.R. BOWEN and P.B. PRANGNELL, Acta Mater. 51, (2003), p.2811.
8) N. TSUJI, T. TOYODA, Y. MINAMINO, Y. KOIZUMI, T. YAMANE, M. KOMATSU and M. KIRITANI, Mater. Sci. and Eng.A, 350, (2003), p.108.
9) E. HORNBOGEN, U. KODTER, Recrystallization of Two-Phase Alloys. Dr. Riederer Verlag GmbH (1984), p 167.
10) F.J. HUMPHREYS and M. HATHERLY, Recrystallization and Related Annealing Phenomena. UK. Pergamon (1995), p 164.
11) S. CHATTOPADHYAY and C.M. SELLARS, Acta Metall. 30, (1982), p.157.
12) R. SONG, D. PONGE, D. RAABE and R. KASPAR, Acta Mater. 53, (2005), p.845.